RESEARCH ARTICLE

WILEY

Berberine plays a cardioprotective role by inhibiting macrophage Wnt5a/β-catenin pathway in the myocardium of mice after myocardial infarction

Chun-xia Tian[1,2] | Ming-yue Li[1,3] | Xin-xin Shuai[4] | Feng Jiang[5] |
Ya-lan Dong[1] | Yang Gui[1] | Zi-li Zhang[1] | Ren-jie Qin[1] | Zhen-yu Kang[1] |
Lan Lin[1] | Alexey Sarapultsev[6] | Bin Wu[2] | Shan-shan Luo[7] | De-sheng Hu[1,8] 🔟

[1]Department of Integrated Traditional Chinese and Western Medicine, Union Hospital, Tongji Medical College, Huazhong University of Science and Technology, Wuhan, China

[2]Department of Cardiology, Hubei Provincial Hospital of Traditional Chinese Medicine, Wuhan, Hubei, China

[3]Department of Gastroenterology, Zhongda Hospital, Southeast University, Nanjing, China

[4]Department of Cardiology, Union Hospital, Tongji Medical College, Huazhong University of Science and Technology, Wuhan, China

[5]Department of International Education, Tianjin University of Traditional Chinese Medicine, Tianjin, China

[6]Institute of Immunology and Physiology, Ural Branch of the Russian Academy of Science, Ekaterinburg, Russia

[7]Department of Hematology, Union Hospital, Tongji Medical College, Huazhong University of Science and Technology, Wuhan, China

[8]Key Laboratory of Biological Targeted Therapy, The Ministry of Education, Wuhan, China

Correspondence
De-sheng Hu, Department of Integrated Traditional Chinese and Western Medicine, Union Hospital, Tongji Medical College, Huazhong University of Science and Technology, Wuhan 430022 China; Key Laboratory of Biological Targeted Therapy, the Ministry of Education, Wuhan 430022 China.
Email: desheng.hu@hust.edu.cn

Abstract

Myocardial infarction (MI) is one of the diseases with high fatality rate. Berberine (BBR) is a monomer compound with various biological functions. And some studies have confirmed that BBR plays an important role in alleviating cardiomyocyte injury after MI. However, the specific mechanism is unclear. In this study, we induced a model of MI by ligation of the left anterior descending coronary artery and we surprisingly found that BBR significantly improved ventricular remodeling, with a minor inflammatory and oxidative stress injury, and stronger angiogenesis. Moreover, BBR inhibited the secretion of Wnt5a/β-catenin pathway in macrophages after MI, thus promoting the differentiation of macrophages into M2 type. In summary, BBR effectively improved cardiac function of mice after MI, and the potential protective mechanism was associated with the regulation of inflammatory responses and the inhibition of macrophage Wnt5a/β-catenin pathway in the infarcted heart tissues. Importantly, these findings supported BBR as an effective cardioprotective drug after MI.

- -

1 | INTRODUCTION

MI is an event of heart attack, which is due to blockage in the interior walls of the arteries, resulting in reduced blood flow and lack of oxygen supply (Sarkar, Grigg, & Lee, 2021). Heart failure is the most common cardiovascular complication following MI and is intricately linked with the development of post-infarction ventricular remodeling. The structural, functional, and geometric alterations of infarcted and non-infarcted myocardium ultimately lead to chamber dilation and cardiac dysfunction (Zhu, Meng, Yu, Shao, & Shen, 2021). Although there was big progression of therapeutic strategies for MI such as percutaneous coronary intervention and coronary artery bypass grafting, the mortality after MI is still increasing (Wu, Berman, Biery, & Blankstein, 2020). Therefore, it is urgent to discover new drugs to rescue the dying myocardium and its function.

There is growing recognition and experimental evidence that the inflammatory response plays a key role in myocardial injury, repair and remodeling after MI (Frangogiannis, 2014). After occurrence of MI, the ischemic necrosis of myocardial cells triggers aseptic inflammation and promotes the release of inflammatory cytokines and chemokines, which then recruit and activate innate immune cells including neutrophils, monocytes/macrophages, and dendritic cells in and nearby infarct myocardium (Peet, Ivetic, Bromage, & Shah, 2020; Viola, de Jager, & Sluijter, 2021). Neutrophils produce high amount of reactive oxygen species and proteases, deteriorating the injury to local tissues. Subsequently, monocytes are recruited to the infarcted tissue and become tissue macrophages, which engulf the apoptotic cells and debris, contributing to the scar formation. Besides the unspecific inflammation, a growing body of evidence demonstrates that macrophage also modulates the immune responses after MI. Macrophage depletion impairs wound healing and increases left ventricular remodeling after MI in mice (van Amerongen, Harmsen, van Rooijen, Petersen, & van Luyn, 2007). The Ly6C^{high} monocytes derived M1 pro-inflammatory macrophages could exert pathogenic effects by releasing pro-inflammatory cytokines including interleukin-1β (IL-1β) and tumor necrosis factor-α (TNF-α), while M2 macrophages sourcing from the Ly6C^{low} monocytes exert the anti-inflammatory responses to myocardium after MI. By releasing the anti-inflammatory mediators such as interleukin-10 (IL-10), transforming growth factor-β (TGF-β), and vascular endothelial growth factor (VEGF), M2 macrophages inhibit the activity of M1 macrophages (Mentkowski, Euscher, Patel, Alevriadou, & Lang, 2020).

Wnt family has also been implicated in response to cardiac stress and injury. Wnt5a is an evolutionarily conserved protein in the Wnt family, which maintains its homeostasis during embryonic morphogenesis (Reichman et al., 2018). Inhibiting the secretion of Wnt5a in macrophage can block the inflammatory autocrine loop, and drive the transition of macrophage to a M2-like phenotype in *Wls^{fl/fl}*, *Cfms-icre* mice, thereby suppressing excessive inflammation and improving infarction repair (Palevski et al., 2017).

BBR is an isoquinoline alkaloid originally isolated from the Chinese herb Coptis chinensis. Due to the powerful properties of antimicrobial, antioxidant, anti-arrhythmic, and anti-inflammatory activities, an increasing number of studies have highlighted the medicinal usefulness of BBR in diverse fields, including digestive system, nervous system, immune system, and cardiovascular system disorders (Och, Podgorski, & Nowak, 2020; Song, Hao, & Fan, 2020; Xu et al., 2021). In mouse models of MI, BBR was found to ameliorate ischemia/reperfusion injury by reducing cardiomyocyte autophagy and apoptosis, inhibiting adenosine-5' monophosphate kinase activity, and inducing the mitophagy-mediated HIF-1α/BNIP3 pathway (Zhu et al., 2020). Although there have been several studies on BBR in ischemic diseases, the intrinsic therapeutic mechanism still needs to be clarified. Given the vital role of immune dysregulation and Wnt5a protein in the pathogenesis of MI, we sought to address the potential impacts of BBR on heart protection and repair to MI mouse model.

2 | MATERIALS AND METHODS

2.1 | Reagents

Berberine (purity:≥98%) was purchased from Chem Faces (#CFN98049). Malondialdehyde (MDA) assay kit (#A003-1) and Superoxide Dismutase (SOD) assay kit (#A001-3) were purchased from NanJing Jiancheng Bioengineering Institute (Nanjing, China). Antibodies against Wnt5a (#sc-365370) were purchased from Santa-Cruz and were dissolved in primary antibody dilution buffer (#P0023A, Beyotime, Wuhan, China). Antibodies against β-catenin (#51067-2-AP) were provided by the Proteintech Group (Wuhan, China). The annexin V apoptosis detection kit I (#559763) was obtained from BD Biosciences (Franklin Lakes, America). Antibodies used for flow cytometry include anti-CD4 (#470041-32), anti-CD8 (#48–0081-82), and anti-Foxp3 (#35–5773-82), which were purchased from eBiosciences (Carlsbad, America). Antibodies including anti-ROR-γt (#562007), anti-Ly6C (#560592), anti-Ly6G (#560600), anti-CD3 (#533066), anti-CD19 (#550992), anti-CD11b (#562950), anti-CD11c (#558079), anti-F4/80 (#565411), and anti-CD45 (#103108) were purchased from BD Biosciences. Human/Mouse/Rat TGF-β1 ELISA Kit (#EK981-96) and Mouse IL-18 ELISA Kit (#EK218-96) were purchased from Multi Sciences (Hangzhou, China). The Mouse CBA Kits of cytokines were obtained from Biolegend (California, America). TUNEL staining kit (#556547) was purchased from BD Biosciences.

2.2 | Animals and administration

Male C57BL/6 mice (8 weeks old, 20–25 g) were purchased from the Beijing Vital River Laboratory Animal Technology Co., Ltd (Beijing, China). These mice were housed at relatively constant humidity (45–75%), temperature (22 ± 2°C), and 12 hr light–dark cycle in SPF environment. All mice were allowed for 1 week housing before the experiment, and the animal protocol was approved by the Committee for Animal Research of Huazhong University of Science and Technology (Wuhan, China).

For the MI model, the mice were anesthetized with 0.1% pentobarbital sodium lying on the mouse plate. Permanent occlusion by ligation of the left anterior descending (LAD) coronary artery was established as previously described (Kolk et al., 2009). The mice were randomly grouped: sham group, MI group, and BBR group. Since the model induction, the BBR group were given BBR in a gavage dose of 40 mg/kg every day for 14 days, and other mice were gavaged with an equal volume of distilled water.

2.3 | Echocardiography measurement

Two weeks after MI surgery, transthoracic echocardiography was performed to evaluate cardiac function using a VEVO-1100 ultrasound system (VisualSonics). Briefly, mice were lightly anaesthetized via 1% isoflurane inhalation, and heart rates were maintained at 450–550 bpm. The left ventricular diastolic dimension (LVIDD), left ventricular internal dimension systole (LVIDS), left ventricular ejection fraction (LVEF), and left ventricular fraction shortening (LVFS) were averaged and calculated over a minimum of five consecutive cardiac cycles per sample.

2.4 | Histological assessment

The hearts of the mice were isolated and rinsed in $1\times$ ice-cold PBS immediately after the mice were sacrificed, and immersed in 4% paraformaldehyde overnight. The fixed tissues were subsequently embedded in paraffin, and sectioned transversely to 5 μm thickness. Masson staining and acid-Sirius staining were performed to visualize the collagen content according to the manufacturer's instructions. Images were acquired by optical or fluorescence microscope (Olympus, Japan), and were analyzed by Image-Pro Plus 6.0.

2.5 | Quantitative real-time polymerase chain reaction for mRNA

Total RNA was extracted from hearts using RNAiso Plus (#9109; TaKaRa, Dalian, China) according to the manufacturer's protocols. After isolation of RNA, PrimeScript RT Master Mix (#RR036A; TaKaRa, Dalian, China) was used to generate complementary DNAs (cDNAs) of mRNAs. After that, these cDNAs were analyzed to explore expression changes of genes by SYBR Premix Ex Taq (#RR420A; TaKaRa, Dalian, China). The relative expression levels of genes in tissues were normalized to β-actin. The sequences of all primers are listed in Table S1.

2.6 | Cytokine measurement

Cytokine was measured using ELISA Kit and CBA Kit according to the manufacturer's protocol. Briefly, the hearts were isolated and homogenized to obtain the supernatants. Then IL-18 and TGF-β were detected by ELISA Kit, and the cytokines IL-10, TNF-α, IL-6, MIP-1β, and VEGF were measured by CBA Kit.

2.7 | Mouse cardiac lymphocyte isolation

Hearts of mice were isolated and washed with cold PBS with 1 M Hepes to remove the blood. Pooled hearts were cut into fragments, then the fragments were digested in 450 U/ml collagenase I (#C0130, Sigma, Missouri, America), 125 U/ml collagenase XI (#C7657, Sigma, Missouri, America), and 60 U/ml DNase I (#10104159001, Roche, Basel, Switzerland) on an orbital shaker at 100 rpm for 15 min at 37°C. After digestion, the cells were filtered through 100 μm strainer, followed by centrifugation at 1650 rpm for 5 min at 4°C, and resuspended in RPMI-1640 for macrophages isolation and flow cytometric analysis.

2.8 | Mouse cardiac macrophages isolation

The lymphocytes were extracted from the hearts as described above. The cells are cultured in cell Petri dishes, 2 hr later, the macrophages will grow adherently. Then discarded supernatants and washed the cells twice with medium. Cell purity was detected by Flow Cytometry with anti-F4/80 and anti-CD11b. Cardiac macrophages were cultured at 37°C in RPMI-1640 supplemented with fetal bovine serum (10%).

2.9 | Flow cytometry

Flow cytometry was performed as described in previously research (Ji et al., 2019). Briefly, Single cell suspensions were stained with the indicated antibodies diluted by PBS supplemented with 2% FBS and 0.5% BSA for surface markers. For Foxp3 and ROR-γt staining, the cells were stained for surface markers such as anti-CD45 and anti-CD4, followed by fixation and permeabilization with fixation and permeabilization buffer (#88–8,824-00; Thermo Fisher Scientific, America) at room temperature for 30 min. After washed with PBS for three the cells were then stained with anti-Foxp3 and anti-ROR-γt antibodies as instructed. All samples were detected and analyzed by CytoFLEX LX Flow Cytometry System.

2.10 | Western blot analysis

Proteins were fractionated from hearts and cells as described above. After quantified by the BCA protein quantitative kit (#P0286, Beyotime Institute of Biotechnology, Shanghai, China), the proteins were electrophoretically separated on a 10% sodium dodecyl sulfate (SDS)-polyacrylamide gel and transferred to polyvinylidene fluoride membranes (#IPVH00010, Millipore, Massachusetts, America). The proteins of interest were detected using primary antibodies against Wnt5a, β-catenin, and GAPDH. Appropriate secondary antibodies were used with primary antibodies. Protein bands were visualized with Chemiluminescence Imaging System and quantitatively analyzed by imageJ software.

2.11 | Tube formation assay

Human umbilical vein endothelial cells (HUVECs) were obtained from Cell Bank of the Chinese Academy of Science (Shanghai, China) and cultured at 37°C and 5% CO_2 in DMEM supplemented with fetal bovine serum (10%). The Matrigel (#E1270, Sigma, Missouri, America) were spread to a 48-well plate. Then the 3×10^4 HUVECs starved overnight were seeded on Matrigel in monolayer, and the culture supernatants were replaced by the supernatants of mouse cardiac macrophage. The HUVECs continued to be cultured at 37°C and 5% CO_2 and photographed every 2 hr to observe tube formation.

2.12 | Migration ability measurement

The photographing position was marked on the bottom of the 12-well plate with a ruler and a marker in advance, and 5×10^5 HUVECs were added in a single layer in a 12-well plate. After the cells were attached and filled the well bottom, we drew a line through the cells with a sharp material. We washed the cells three times with PBS and added serum-free DMEM. HUVECs were continued to be incubated at 37°C and 5% CO_2, and cell migration was photographed and recorded every 6 hr.

2.13 | Oxidative stress detection

H9C2 cells were obtained from the American Type Culture Collection (ATCC, VA, USA). Cells were cultured in monolayer at 37°C and 5% CO_2 in DMEM supplemented with fetal bovine serum (10%). 5×10^5 H9C2 cells were added to a 12-well plate. After the treatments with H_2O_2 and BBR, the H9C2 cells were collected to detect the levels of oxidative stress by MDA assay kit and SOD assay kit according to the instructions.

2.14 | Apoptosis measurement

H9C2 cells were cultured in monolayer at 37°C and 5% CO_2 in DMEM supplemented with fetal bovine serum (10%). 5×10^5 H9C2 cells were added to a 12-well plate. After the treatments with H2O2 and BBR, the level of apoptosis in H9C2 cells was detected by TUNEL staining kit according to the instructions.

2.15 | Statistical analysis

All the data were presented as mean ± S.E.M, and statistics were analyzed with GraphPad Prism (GraphPad Prism version 6.0). The data of RT-PCR were normalized to control to avoid unwanted sources of variation. Student's t-tests were used to compare the means of two groups, and one-way ANOVA with Tukey's test was used to compare the means among multiple groups. $p < 0.05$ were considered significant. Statistical analysis is indicated in each figure legend.

3 | RESULTS

3.1 | BBR improves cardiac function and inhibits ventricular remodeling after MI in mice

Echocardiography results showed that LVIDD and LVIDS of mice treated with BBR were significantly lower than those of the model group ($p < .05$), while LVEF and LVFS were significantly higher than those of model group ($p < .05$); (Figure 1a,b), suggesting the cardioprotective effect of BBR. Next, we evaluated the body weights (BW) and the ratios of heart weight (HW) to BW of the mice. The data showed that both the BW and HW/BW ratios were increased in the MI group ($p < .05$), indicating the enlarged heart of the mouse of the MI group, while BBR administration could significantly reverse the change ($p < .05$); (Figure 1c,d). Then, we evaluated the effect of BBR on pathological changes of heart. We performed the Sirius red staining and Masson's trichrome staining on the infarcted heart tissues from each group. The results showed that the size of heart collagen fiber area was significantly reduced in mice after BBR treatment compared with those in the MI model group ($p < .01$); (Figure 1e,f, S1A), suggesting the function of BBR in reversing the ventricular remodeling. Overall, these data demonstrated that BBR performs a cardioprotective function and inhibit the ventricular remodeling after MI.

3.2 | BBR orchestrates an antiinflammatory immune response in infarcted myocardium of MI mice

Here, we investigated these innate immune cells by flow cytometry, and the gating strategy is shown in Figure 2a. Further analysis showed that neutrophils were significantly increased in infarcted heart tissue of the MI group ($p < .05$). However, BBR treatment reversed the change ($p < .05$); (Figure 2b). Although there was no significant difference in cell numbers of total heart macrophages among the three groups, BBR reduced the absolute number of pro-inflammatory Ly6C^{high} macrophages ($p < .01$), while increased the anti-inflammatory Ly6C^{low} macrophages in heart tissues compared with the MI model
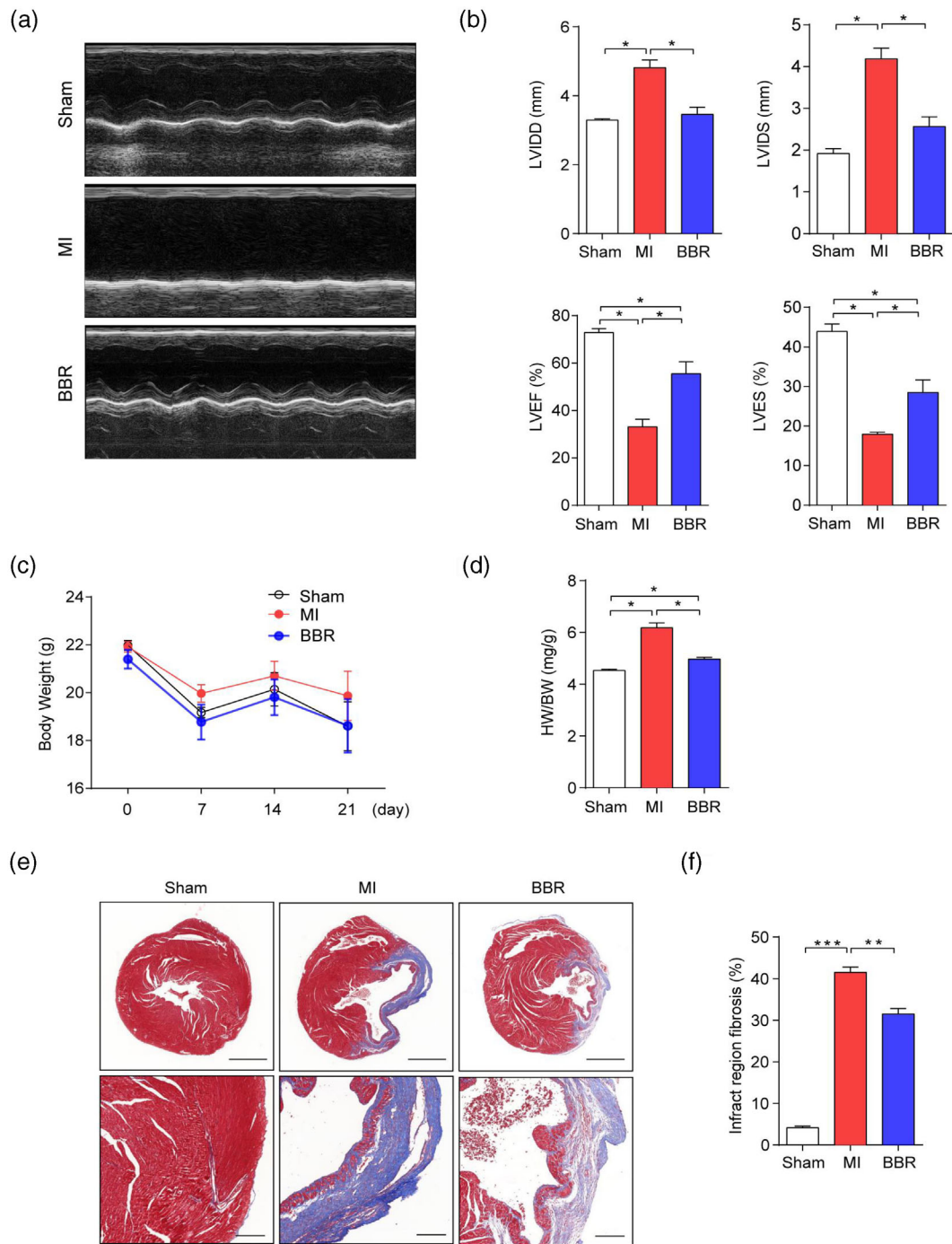
FIGURE 1 Berberine can improve cardiac function and inhibit ventricular remodeling after Myocardial infarction (MI) in mice.
(a) Representative echocardiography images of sham group, MI group, and Berberine group. (b) left ventricular diastolic dimension, left ventricular internal dimension systole, left ventricular ejection fraction, and left ventricular fraction shortening were measured by echocardiography. (c) Body weight changes of each group. (d) The ratio of heart weight to body weight of mice in each group. (e) Representative Masson staining (Bar = 1 mm above, Bar = 200um below) sections and (f) the percentage of infarct region fibrosis of mice in each group. $n = 6$ animals per group. Data are presented as mean ± SEM. *$p < .05$, **$p < .01$, ***$p < .001$

group ($p < .05$); (Figure 2b). However, the above phenotypes were not observed in the spleen and LNs (Figure S1b). These results indicated that BBR inhibited the neutrophil recruitment of infarcted myocardium and preferentially promoted the polarization of monocytes to Ly6C^{low} macrophages in the heart of mice after MI and play a cardioprotective role in the process of MI.

As the main participating cells of cellular immunity, T cells were also analyzed by flow cytometry, and the gating strategy is shown in Figure S1c. The data showed that the numbers of total CD4$^+$ T cells and CD8$^+$ T cells had no significant difference among three groups. Compared with the MI model group, the number of CD4$^+$Foxp3$^+$ Treg cells was significantly increased in the heart ($p < .05$), spleen
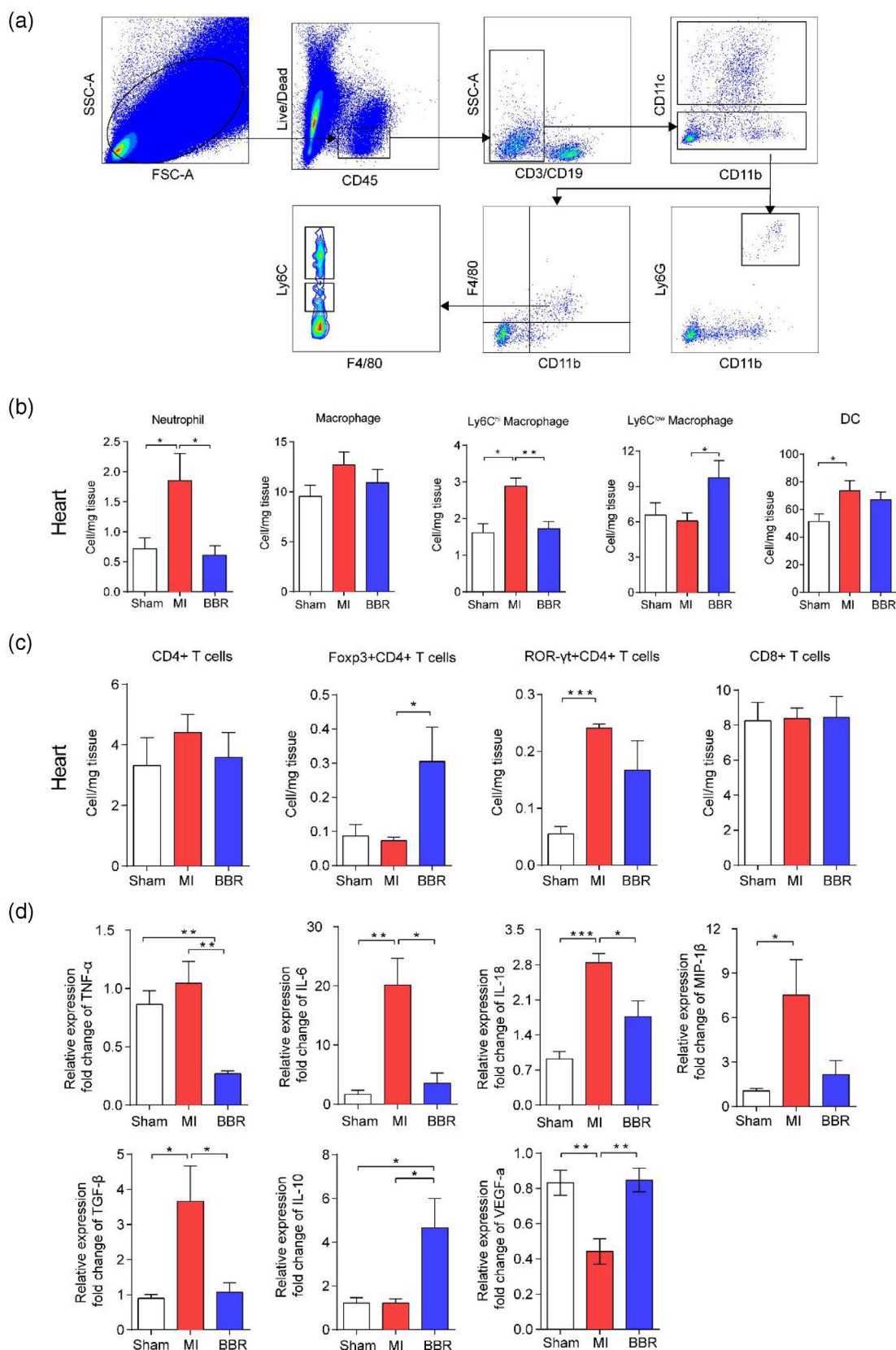
FIGURE 2 Berberine plays a cardioprotective role by mediating the immune cells and cytokines in mice with Myocardial infarction (MI). (a) Flow cytometry gating strategies for each cell population. (b) The bar charts show the percentages of neutrophils, Macrophages, Ly6C^{high} macrophages, Ly6C^{low} macrophages, DCs, (c) and CD4$^+$ T cells, Foxp3$^+$CD4$^+$ Treg cells, ROR-γt$^+$CD4$^+$ T, and CD8$^+$ T cells by flow cytometry. (d) The mRNA expression of TNF-α, IL-6, IL-18, MIP-1β, TGF-β, IL-10, VEGF-α by RT-PCR, using infarcted heart tissues from the sham group, MI group, and Berberine group. $n = 6$ animals per group. Data are presented as mean ± *SEM*. *$p < .05$, **$p < .01$, ***$p < .001$

($p < .05$) and LNs ($p < .05$) of mice treated with BBR, and the number of CD4^{+}ROR-γt^{+} Th17 cells in the heart showed a trend of decrease but there was no significant difference (Figure 2c, S1d). Treg cells act as regulatory cells to suppress the immune response, and thus increased Treg cells and protect the heart from damage. The data further confirmed that BBR can reduce the inflammatory response after MI in mice.

Cytokines are also the important players in the inflammatory responses after MI. Here, we examined the mRNA levels of inflammation-related factors of the infarcted tissues by RT-PCR. The mRNA expression of pro-inflammatory factors TNF-α ($p < .01$), IL-6 ($p < .05$), IL-18 ($p < .05$), and TGF-β ($p < .05$) was significantly decreased, and the expression of anti-inflammatory factors IL-10 ($p < .05$) was increased in heart tissues of mice treated with BBR compared with those in the MI group (Figure 2d). In addition, the expression of VEGF was also increased in the BBR group compared with those in the MI group ($p < .01$); (Figure 2d). These results revealed that BBR could inhibit the inflammatory responses in the myocardium and thus prevent the damage to heart of MI mice.

3.3 | BBR alleviates oxidative damage and reduces inflammation in vitro

In order to verify the effect of BBR in vitro, oxidative damage model was established in H9C2 cells and HUVECs. The results showed that BBR could reduce intracellular oxidative damage, and maintain the normal cell morphology, which was due to the decreased intracellular MDA ($p < .05$) and SOD ($p < .05$); (Figure 3a,b). Next, we examined the apoptotic status of H9C2 cells by staining annexin V and 7-AAD, and it showed that 5.0 uM BBR could potentially prevent early apoptosis ($p < .05$); (Figure 3c). In addition, we examined the migration and angiogenesis ability of HUVECs in wound healing experiment. The result demonstrated that 2.5 uM BBR could promote the migration of HUVECs after hypoxia treatment ($p < .05$); (Figure 3d). All together, these data indicate that BBR could inhibit the apoptosis of H9C2 cells and promote the migration of HUVECs after hypoxia injury, thus demonstrating its cardioprotective effect after MI.

3.4 | BBR alleviates MI in mice by inhibiting Wnt5a/β-catenin pathway

To further investigate the mechanism of BBR's cardioprotective effect after MI, we detected the expression of Wnt5a and β-catenin in infarcted heart tissue. The data showed that both the protein and mRNA levels ($p < .001$) of Wnt5a increased and the expression of β-catenin slightly decreased in the hearts of mice after MI, whereas BBR could reverse this phenotype ($p < .001$); (Figure 4a,b). To determine the cell types that contribute to the upregulated Wnt5a, we extracted and in vitro cultured mouse immune cells for macrophage selection. The upregulated Wnt5a and downregulated β-catenin were detected in the MI group, and BBR could reverse the phenotypes

(Figure 4c,d). These data confirm the above results, suggesting that macrophages derived from Wnt5a/β-catenin signaling may play the important role in MI. In addition, we also verified the function of macrophages in angiogenesis in tube formation experiment, and we found that the macrophage supernatant in BBR group could significantly enhance the angiogenesis of HUVECs ($p < .05$) when co-cultured with HUVECs (Figure 4e).

In order to further investigate the role of Wnt5a/β-catenin in MI, we gave intraperitoneal injection of BBR or FH535, the inhibitor of Wnt/β-catenin, to mice after MI. The echocardiography data demonstrated that, compared with MI group, both BBR and FH535 administration could significantly downregulate LVIDD (all $p < .001$) and LVIDS (all $p < .01$) to similar levels, and upregulate LVEF ($p < .01$) and LVFS levels with better function of FH535 when compared with BBR ($p < .01$); (Figure.4f). These data revealed that BBR harbors similar function as the inhibitor against Wnt5a/β-catenin signaling pathway, and its cardioprotective function might be due to the inhibition of the Wnt5a/β-catenin pathway.

4 | DISCUSSION

MI is an urgent clinical event due to formation of plaques in the interior walls, and the immune response to MI is essential for cardiac repair and also affects the process of post-infarction remodeling and heart failure. Our current studies demonstrated that BBR administration restored cardiac function by rebalancing the immune homeostasis, and inhibiting Wnt5a/β-catenin pathway in the infarcted heart.

Cardiomyocyte injury, myocardial fibrosis, and cardiac dysfunction are the characteristics of the pathological changes after MI. Previous studies revealed that BBR inhibits cardiac remodeling of heart failure after MI by reducing myocardial cell apoptosis in rat model (Liao et al., 2018). Other studies also showed that BBR promoted cardiac function by upregulating PINK1/Parkin-mediated mitophagy in heart failure (Abudureyimu et al., 2020), and by attenuating cell apoptosis by activating AK2/STAT3 signaling pathway (Zhao et al., 2016). These data demonstrate that BBR could play a protective role in ischemia or hypoxia. In our study, BBR treatment significantly improved cardiac function and inhibited ventricular remodeling after MI by echocardiographic and histological assay, confirming previous findings.

During MI, inflammatory response is a double-edged sword because it is essential for cardiac repair, but also implicated in the pathogenesis of post-infarction remodeling and heart failure. Expressions of the pro-inflammatory cytokines TNF, IL-1β, and IL-18 increased significantly in the experimental models of MI (Toldo & Abbate, 2018; Viola et al., 2021, 2021). TNF is released after MI and can promote the inflammatory injury, inducing Ca^{2+}-influx in cardiomyocytes (Bartekova, Radosinska, Jelemensky, & Dhalla, 2018), and anti-TNF-α treatment reduced the levels of inflammatory cytokines and the inflammatory cells in and around the infarct area (Wang, Guo, Ding, & Mehta, 2018). As another pro-inflammatory cytokine, IL-18 regulates cardiomyocyte hypertrophy and induces extracellular matrix
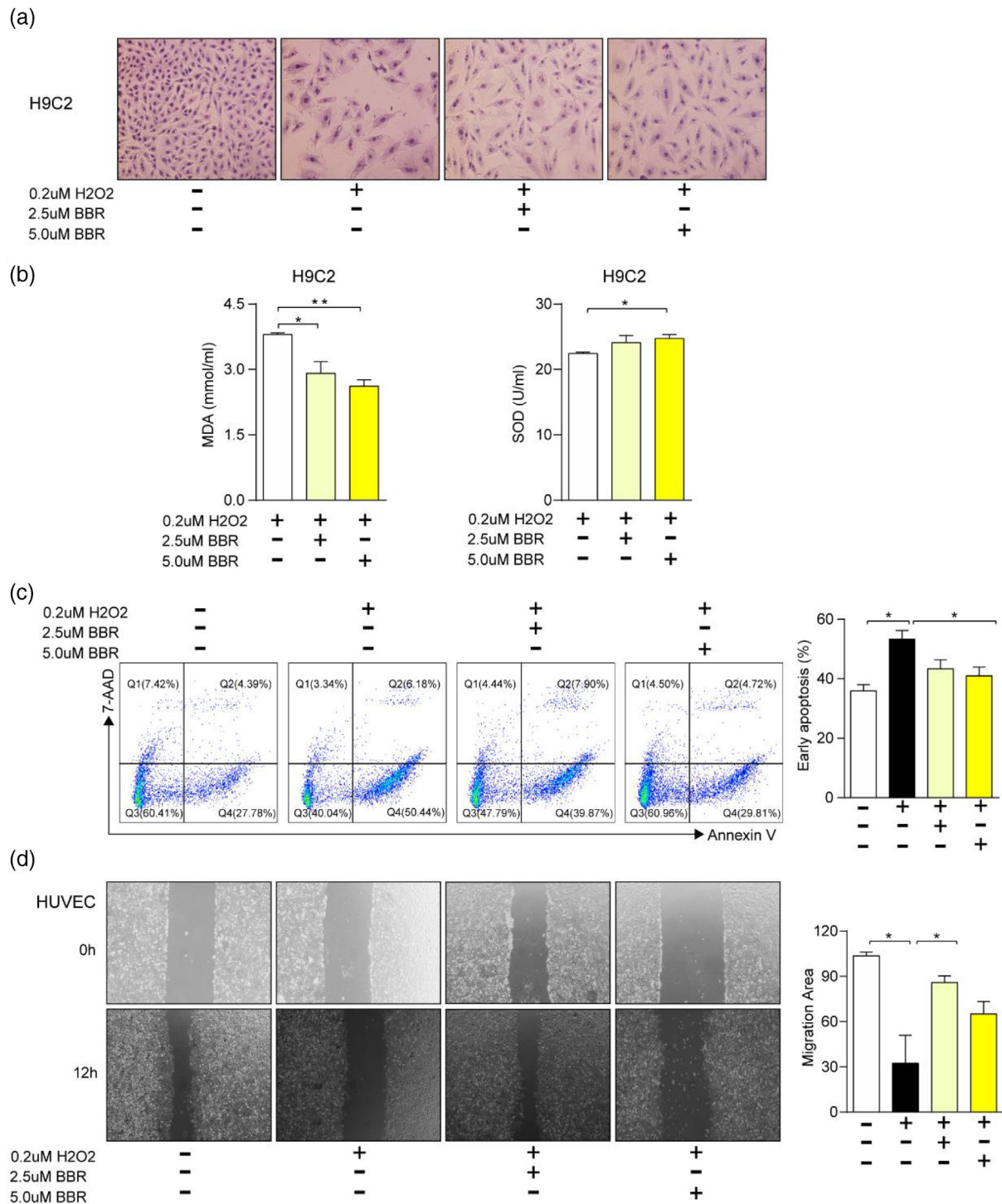
FIGURE 3 Berberine can alleviate oxidative damage of H9C2 and improve the migration and angiogenesis ability of HUVEC. H9C2 cells were administrated with H_2O_2, and low or high dose of Berberine (BBR) under the condition of hypoxia injury, (a) the morphology of the cells was observed, (b) the concentrations of malondialdehyde and superoxide dismutase, (c) the staining of 7-AAD/Annexin V (left), and the percentages of early apoptotic cells (right) were measured in these cells. (d) The migration ability of HUVECs was assayed (left) and the migration area was calculated (right) under the condition of hypoxia injury and the treatment of H_2O_2 and different concentration of BBR. Data are presented as mean ± SEM. *$p < .05$, **$p < .01$, ***$p < .001$

remodeling and cardiac contractile dysfunction (O'Brien et al., 2014; Wang et al., 2009). Persistent inflammation induces adverse effects on heart functions and remodeling after MI. IL-10, a traditional anti-

inflammatory cytokine, inhibits inflammation and reduces heart remodeling after MI (Jung et al., 2017; Shirakawa et al., 2018). After MI, BBR administration ameliorated the secretion of pro-inflammatory
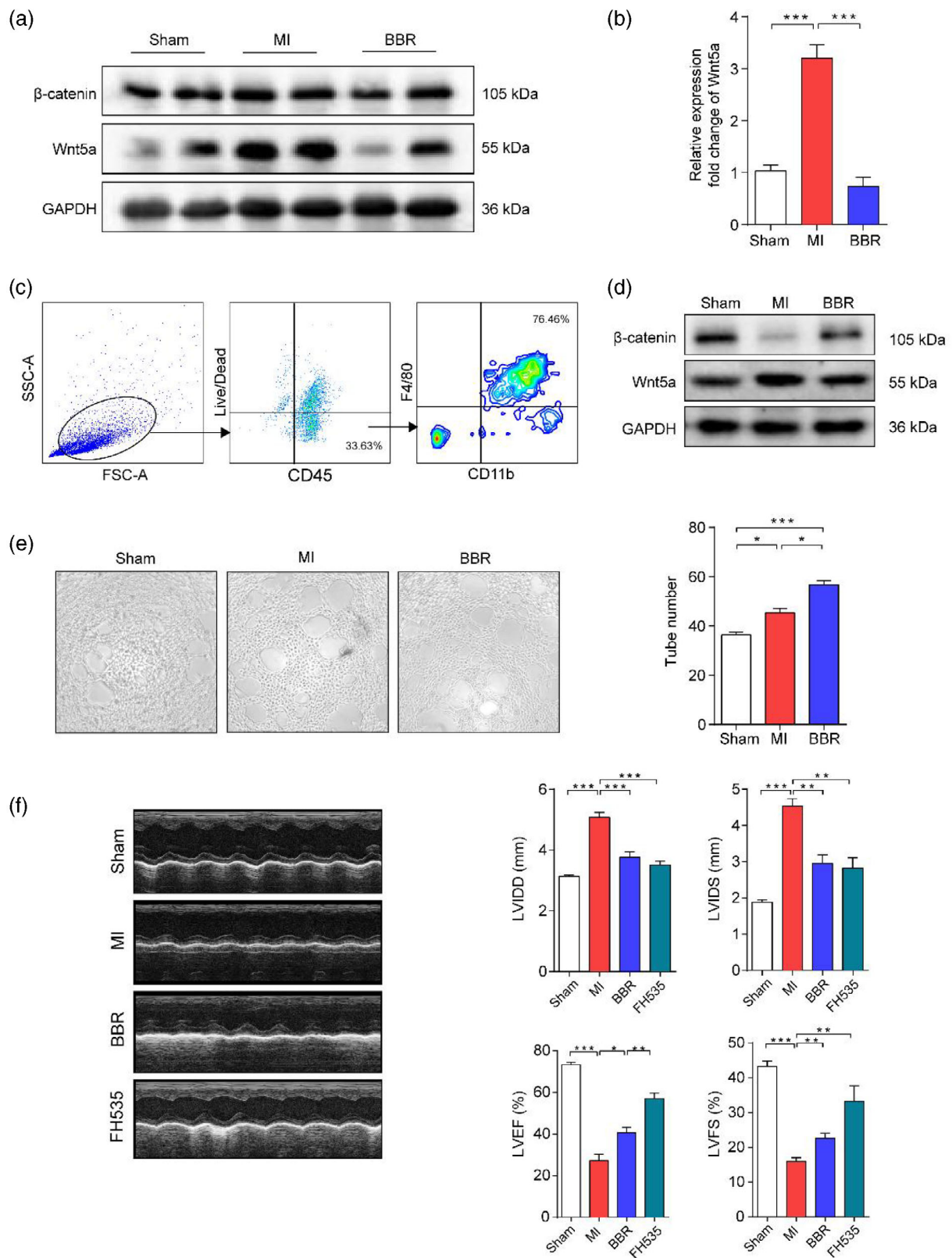
FIGURE 4 Berberine alleviates MI in mice by inhibiting Wnt5a pathway. (a-b) Infarcted heart tissues from sham, Myocardial infarction (MI), and Berberine (BBR) groups were collected for protein and mRNA preparation. The protein levels of Wnt5a and β-catenin and mRNA level of Wnt5a were measured by western blotting and PCR, respectively. Lymphocytes were prepared from heart tissues of three groups, and cultured for macrophage selection. (c) The extracted cardiac macrophages were evaluated by flow cytometry, (d) and the protein levels of Wnt5a and β-catenin were assayed by western blotting. The effect of cardiac macrophages on angiogenesis was evaluated by tube formation experiment co-cultured with supernatant of cultured macrophages. (e) The images and numbers of formed tubes were examined. (f) The pictures show the representative echocardiography images, and the bar charts indicate the levels of left ventricular diastolic dimension, left ventricular internal dimension systole, left ventricular ejection fraction, and left ventricular fraction shortening from sham, MI, BBR, and FH535 groups. $n = 5$ animals per group. Data are presented as mean ± *SEM*. *$p < .05$, **$p < .01$, ***$p < .001$

cytokine TNF-α, IL-18, and TGF-β, and up-regulated the expression of the anti-inflammatory cytokine IL-10, thus protecting the myocardium from damage due to excessive immune responses.

To resolve the ischemic status after MI, pro-angiogenesis and building up the traffic branch are regarded as the effective approaches for ischemic heart disease. VEGF is a strong and essential proangiogenic factor and plays an important role in angiogenesis (Zou et al., 2019). The data showed that BBR promoted the expression of VEGF and thus induced angiogenesis in the infarcted heart.

Innate and adaptive immune cells are involved in the process of MI. Following MI, peripheral and resident innate immune cells such as neutrophils, monocytes, macrophages rapidly recruit and coordinate their function to initiate the inflammatory responses, and promote tissue damage and remodeling. Neutrophils are recruited to the infarcted myocardium at the early stage, and the secreted proteases induce inflammatory responses (Ogura et al., 2021). Monocytes/macrophages are critical players in the initial inflammatory response to injury and subsequent would healing in infarcted myocardium (Wright, FitzPatrick, & Firth, 2018). Pro-inflammatory M1 and reparative M2 macrophages originate from the circulating Ly6C^{high} and Ly6C^{low} monocytes, respectively (Ma, Mouton, & Lindsey, 2018). M1 macrophages are the predominant population early post-MI, peaking between Days 3 and 5, performing a pro-inflammatory function including TNF-α expression and high proteinase activity. When inflammation resolves, M2 macrophages predominate, peaking on day 7 after MI (Peet et al., 2020, 2020). Studies have shown that BBR promoted monocyte polarization toward M2 macrophages in several disease models (Gao et al., 2021; Han et al., 2020; Yang et al., 2021). In addition, Foxp3$^+$CD4$^+$ Treg cells were also significantly increased. Besides the function of immune suppression, Foxp3$^+$CD4$^+$ T cells also improve healing after MI by modulating monocyte differentiation, suggesting the beneficial effect on cardiac healing post-MI (Weirather et al., 2014). Our data showed that the number of pro-inflammatory

Ly6C^{high} monocytes was significantly reduced and Ly6C^{low} monocytes increased in the infarcted heart of BBR-treated group compared with MI model group. These data revealed the critical cardioprotective role of BBR post-MI.

Oxidative stress is believed to contribute to the pathogenesis of many diseases. After MI, oxidative stress is formed in both infarcted and nearby myocardium, and myocardial damage caused by oxidative stress has been regarded as an obstructive factor on recovery after MI (Tomandlova et al., 2021). In this study, the data verified the function of BBR in alleviating oxidative stress and oxidative damage in cultured cells, suggesting the strong cardio-protective role.

Wnt/β-catenin signaling pathway is essential for embryo development and adult tissue homeostasis and regeneration. This pathway plays a critical role in response to heart injury. Previous experiments showed that Wnt/β-catenin signaling pathway promoted fibrosis and cardiac remodeling in myocardium, and targeting the Wnt in myocardium was believed to improve and repair ischemic heart (Haybar, Khodadi, & Shahrabi, 2019). In this study, we were surprised to find that BBR reduced the expression of Wnt5a protein in the heart after MI, while β-catenin protein expression showed the opposite trend. Further experiments demonstrated that macrophage-derived Wnt5a/β-catenin probably played the roles in cardio-protection. More interestingly, when we compared BBR with Wnt5a inhibitor FH535 in MI mice, the heart function of the mice were significantly improved on both groups of mice treated with BBR or FH535. Therefore, we concluded that BBR can inhibit the inflammatory response and reduce the cardiac injury after MI by inhibiting the Wnt5a/β-catenin pathway.

In this study, our data showed that BBR promotes monocyte polarization toward M2 macrophage, inhibits the secretion of pro-inflammatory factors, and reduces ventricular remodeling, thus demonstrating its protective effect on cardiac function of infarcted heart (Figure 5). Further study also demonstrated that the protective effect
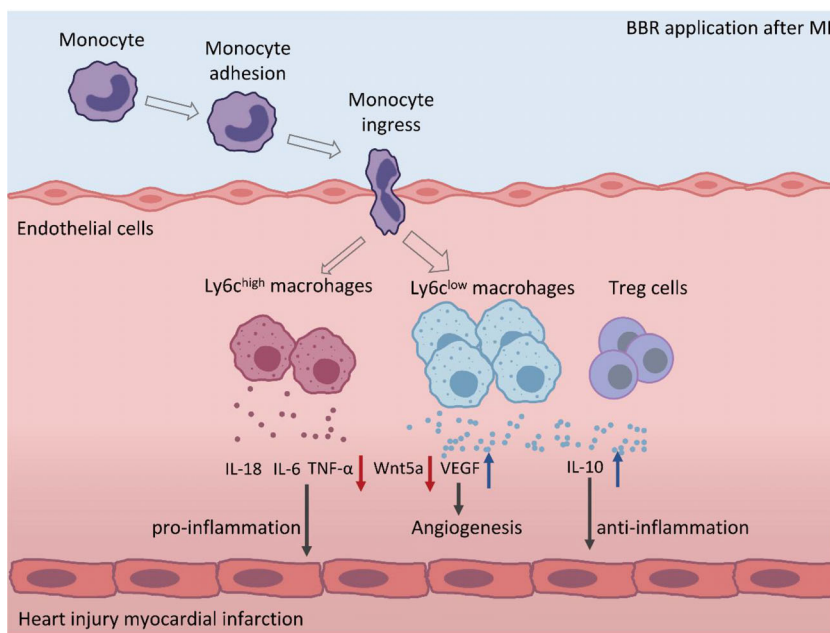

FIGURE 5 Schematic depiction of alteration of the immune homeostasis after Berberine (BBR) application in Myocardial infarction. Mechanism diagram of BBR regulating the immunity of mice after myocardial infarction by inhibiting Wnt5

can be reversed after administering Wnt5a inhibitor. These data provide solid evidence of BBR in implementing the cardioprotective role by inhibiting Wnt5a/β-catenin pathway in heart after MI.

AUTHOR CONTRIBUTIONS

De-sheng Hu, **Chun-xia Tian**, **Ming-yue Li**, and **Xin-xin Shuai** conceived the project. **De-sheng Hu**, **Zhen-yu Kang**, and **Lan Lin** secured the funding. **Chun-xia Tian**, **Ming-yue Li**, and **Xin-xin Shuai** designed and performed the experiments. **Feng Jiang**, **Ya-lan Donga**, **Yang Gui**, **Zi-li Zhang**, **Ren-jie Qin**, **Zhen-yu Kang**, **Lan Lin**, **Alexey Sarapultsev**, **Bin Wu**, and **Shan-shan Luo** analyzed the data. **De-sheng Hu** provided critical discussion, editing and final approval of the manuscript.

ACKNOWLEDGEMENTS

CONFLICT OF INTEREST

All authors declare no conflict of interest.

DATA AVAILABILITY STATEMENT

The data that support the findings of this study are available from the corresponding author upon reasonable request.

ETHICS STATEMENT

The study was approved by the Laboratory Animal Ethics Committee of Tongji Medical College of Huazhong University of Science and Technology and performed in accordance with the guidelines prescribed by the committee.

ORCID

De-sheng Hu 🄳 https://orcid.org/0000-0002-9608-0310

REFERENCES

Abudureyimu, M., Yu, W., Cao, R. Y., Zhang, Y., Liu, H., & Zheng, H. (2020). Berberine promotes cardiac function by upregulating PINK1/Parkin-mediated Mitophagy in heart failure. *Frontiers in Physiology*, *11*, 565751.

Bartekova, M., Radosinska, J., Jelemensky, M., & Dhalla, N. S. (2018). Role of cytokines and inflammation iin heart function during health and disease. *Heart Failure Reviews*, *23*, 733–758.

Frangogiannis, N. G. (2014). The inflammatory response in myocardial injury, repair, and remodelling. *Nature Reviews. Cardiology*, *11*, 255–265.

Gao, Z. S., Zhang, C. J., Xia, N., Tian, H., Li, D. Y., Lin, J. Q., ... Wu, C. (2021). Berberine-loaded M2 macrophage-derived exosomes for spinal cord injury therapy. *Acta Biomaterialia*, *126*, 211–223.

Han, Y. B., Tian, M., Wang, X. X., Fan, D. H., Li, W. Z., Wu, F., & Liu, L. (2020). Berberine ameliorates obesity-induced chronic inflammation through suppression of ER stress and promotion of macrophage M2 polarization at least partly via downregulating lncRNA Gomafu. *International Immunopharmacology*, *86*, 106741.

Haybar, H., Khodadi, E., & Shahrabi, S. (2019). Wnt/beta-catenin in ischemic myocardium: Interactions and signaling pathways as a therapeutic target. *Heart Failure Reviews*, *24*, 411–419.

Ji, J., Ge, X., Chen, Y., Zhu, B., Wu, Q., Zhang, J., ... Shi, L. (2019). Daphnetin ameliorates experimental colitis by modulating microbiota composition and Treg/Th17 balance. *The FASEB Journal*, *33*(8), 9308–9322.

Jung, M., Ma, Y., Iyer, R. P., DeLeon-Pennell, K. Y., Yabluchanskiy, A., Garrett, M. R., & Lindsey, M. L. (2017). IL-10 improves cardiac remodeling after myocardial infarction by stimulating M2 macrophage polarization and fibroblast activation. *Basic Research in Cardiology*, *112*, 33.

Kolk, M. V., Meyberg, D., Deuse, T., Tang-Quan, K. R., Robbins, R. C., Reichenspurner, H., & Schrepfer, S. (2009). LAD-ligation: A murine model of myocardial infarction. *Journal of Visualized Experiments*, *32*, 1438.

Liao, Y., Chen, K., Dong, X., Li, W., Li, G., Huang, G., ... Fang, Y. (2018). Berberine inhibits cardiac remodeling of heart failure after myocardial infarction by reducing myocardial cell apoptosis in rats. *Experimental and Therapeutic Medicine*, *16*, 2499–2505.

Ma, Y., Mouton, A. J., & Lindsey, M. L. (2018). Cardiac macrophage biology in the steady-state heart, the aging heart, and following myocardial infarction. *Translational Research*, *191*, 15–28.

Mentkowski, K. I., Euscher, L. M., Patel, A., Alevriadou, B. R., & Lang, J. K. (2020). Monocyte recruitment and fate specification after myocardial infarction. *American Journal of Physiology. Cell Physiology*, *319*, C797–C806.

O'Brien, L. C., Mezzaroma, E., Van Tassell, B. W., Marchetti, C., Carbone, S., Abbate, A., & Toldo, S. (2014). Interleukin-18 as a therapeutic target in acute myocardial infarction and heart failure. *Molecular Medicine*, *20*, 221–229.

Och, A., Podgorski, R., Nowak, R., 2020. Biological activity of Berberine-a summary update. Toxins (Basel), *12*, 713.

Ogura, Y., Tajiri, K., Murakoshi, N., Xu, D., Yonebayashi, S., Li, S., ... Ieda, M. (2021). Neutrophil elastase deficiency ameliorates myocardial injury post myocardial infarction in mice. *International Journal of Molecular Sciences*, *22*, 722.

Palevski, D., Levin-Kotler, L. P., Kain, D., Naftali-Shani, N., Landa, N., Ben-Mordechai, T., ... Leor, J. (2017). Loss of macrophage Wnt secretion improves remodeling and function after myocardial infarction in mice. *Journal of the American Heart Association*, *6*, e004387.

Peet, C., Ivetic, A., Bromage, D. I., & Shah, A. M. (2020). Cardiac monocytes and macrophages after myocardial infarction. *Cardiovascular Research*, *116*, 1101–1112.

Reichman, D. E., Park, L., Man, L., Redmond, D., Chao, K., Harvey, R. P., ... James, D. (2018). Wnt inhibition promotes vascular specification of embryonic cardiac progenitors. *Development*, *145*, dev159905.

Sarkar, A., Grigg, W. S., & Lee, J. J. (2021). *TIMI grade flow*. Treasure Island (FL): StatPearls.

Shirakawa, K., Endo, J., Kataoka, M., Katsumata, Y., Yoshida, N., Yamamoto, T., ... Sano, M. (2018). IL (interleukin)-10-STAT3-Galectin-3 Axis is essential for Osteopontin-producing reparative macrophage polarization after myocardial infarction. *Circulation*, *138*, 2021–2035.

Song, D., Hao, J., & Fan, D. (2020). Biological properties and clinical applications of berberine. *Frontiers in Medicine*, *14*, 564–582.

Toldo, S., & Abbate, A. (2018). The NLRP3 inflammasome in acute myocardial infarction. *Nature Reviews. Cardiology*, *15*, 203–214.

Tomandlova, M., Parenica, J., Lokaj, P., Ondrus, T., Kala, P., Miklikova, M., ... Tomandl, J. (2021). Prognostic value of oxidative stress in patients with acute myocardial infarction complicated by cardiogenic shock: A prospective cohort study. *Free Radical Biology & Medicine*, *174*, 66–72.

van Amerongen, M. J., Harmsen, M. C., van Rooijen, N., Petersen, A. H., & van Luyn, M. J. (2007). Macrophage depletion impairs wound healing

and increases left ventricular remodeling after myocardial injury in mice. *The American Journal of Pathology*, 170, 818–829.

Viola, M., de Jager, S. C. A., & Sluijter, J. P. G. (2021). Targeting inflammation after myocardial infarction: A therapeutic opportunity for extracellular vesicles? *International Journal of Molecular Sciences*, 22, 7831.

Wang, X., Guo, Z., Ding, Z., & Mehta, J. L. (2018). Inflammation, autophagy, and apoptosis after myocardial infarction. *Journal of the American Heart Association*, 7 ， e008024.

Wang, M., Tan, J., Wang, Y., Meldrum, K. K., Dinarello, C. A., & Meldrum, D. R. (2009). IL-18 binding protein-expressing mesenchymal stem cells improve myocardial protection after ischemia or infarction. *Proceedings of the National Academy of Sciences of the United States of America*, 106, 17499–17504.

Weirather, J., Hofmann, U. D., Beyersdorf, N., Ramos, G. C., Vogel, B., Frey, A., … Frantz, S. (2014). Foxp3+ CD4+ T cells improve healing after myocardial infarction by modulating monocyte/macrophage differentiation. *Circulation Research*, 115, 55–67.

Wright, C. F., FitzPatrick, D. R., & Firth, H. V. (2018). Paediatric genomics: Diagnosing rare disease in children. *Nature Reviews. Genetics*, 19, 253–268.

Wu, W. Y., Berman, A. N., Biery, D. W., & Blankstein, R. (2020). Recent trends in acute myocardial infarction among the young. *Current Opinion in Cardiology*, 35, 524–530.

Xu, X., Yi, H., Wu, J., Kuang, T., Zhang, J., Li, Q., … Fan, G. (2021). Therapeutic effect of berberine on metabolic diseases: Both pharmacological data and clinical evidence. *Biomedicine & Pharmacotherapy*, 133, 110984.

Yang, T., Wang, R., Liu, H., Wang, L., Li, J., Wu, S., … Zhao, Y. (2021). Berberine regulates macrophage polarization through IL-4-STAT6 signaling pathway in helicobacter pylori-induced chronic atrophic gastritis. *Life Sciences*, 266, 118903.

Zhao, G. L., Yu, L. M., Gao, W. L., Duan, W. X., Jiang, B., Liu, X. D., … Wang, Y. (2016). Berberine protects rat heart from ischemia/reperfusion injury via activating JAK2/STAT3 signaling and attenuating endoplasmic reticulum stress. *Acta Pharmacologica Sinica*, 37, 354–367.

Zhu, N., Li, J., Li, Y., Zhang, Y., Du, Q., Hao, P., … Li, L. (2020). Berberine protects against simulated ischemia/reperfusion injury-induced H9C2 Cardiomyocytes apoptosis in vitro and myocardial ischemia/reperfusion-induced apoptosis in vivo by regulating the Mitophagy-mediated HIF-1alpha/BNIP3 pathway. *Frontiers in Pharmacology*, 11, 1367.

Zhu, F., Meng, Q., Yu, Y., Shao, L., & Shen, Z. (2021). Adult Cardiomyocyte proliferation: A new insight for myocardial infarction therapy. *Journal of Cardiovascular Translational Research*, 14, 457–466.

Zou, J., Fei, Q., Xiao, H., Wang, H., Liu, K., Liu, M., … Wang, N. (2019). VEGF-A promotes angiogenesis after acute myocardial infarction through increasing ROS production and enhancing ER stress-mediated autophagy. *Journal of Cellular Physiology*, 234, 17690–17703.

SUPPORTING INFORMATION

Additional supporting information can be found online in the Supporting Information section at the end of this article.